# FACILE FABRICATION OF C<sub>03</sub>O<sub>4</sub>/ITO ELECTRODE VIA ELECTROPHORETIC DEPOSITION FOR ELECTROCHEMICAL DETECTION OF Pb(II)

Tran Thi Thanh Lam<sup>1</sup>, Trieu Thi Anh<sup>1</sup>, Ma Thi Binh<sup>2</sup>, Tran Quoc Toan<sup>1</sup>, Nguyen Quoc Dung<sup>1\*</sup>

<sup>1</sup>TNU - University of Education, <sup>2</sup>Yen Lam Secondary School – Tuyen Quang

ARTICLE INFO		ABSTRACT			
Received:	26/6/2025	In this study, a simple and cost-effective method was developed to			
Revised:	20/8/2025	fabricate a Co <sub>3</sub> O <sub>4</sub> /ITO electrode through a three-step process: chemical precipitation of Co(OH) <sub>2</sub> from a Co(NO <sub>3</sub> ) <sub>2</sub> solution, electrophoretic			
Published:	20/8/2025	deposition onto an ITO substrate, and low-temperature annealing at			
KEYWORDS		$300^{\circ}\text{C}$ to convert $\text{Co(OH)}_2$ into $\text{Co}_3\text{O}_4$ . The resulting $\text{Co}_3\text{O}_4$ nanostructure exhibited promising electrochemical activity for the detection of Pb(II) ions in aqueous solution. Differential pulse anodic stripping voltammetry was used to evaluate the sensor performance. The accumulation potential and time were systematically optimized, with the best values found to be $-0.9\text{V}$ and $300\text{s}$ , respectively. Under			
					Cobalt oxide
Electrochemical sensor					
Pb(II)					
Chemical precipitation					these conditions, the sensor exhibited a linear current response to Pb(II) concentrations in the range of 0.01 to $2\mu M$ , with a sensitivity of $35.72\mu Acm^{-2}.\mu M^{-1}$ and a detection limit of 0.0047 $\mu M$ . Despite the simplicity of the fabrication method, the sensor demonstrated high performance, indicating its potential for the electrochemical detection of heavy metal ions in environmental monitoring.
Electrophoretic deposition					

# PHƯƠNG PHÁP ĐƠN GIẢN CHẾ TẠO ĐIỆN CỰC $C_{03}O_4$ /ITO THÔNG QUA PHƯƠNG PHÁP LẮNG ĐỘNG ĐIỆN DI TRONG CẢM BIẾN ĐIỆN HÓA PHÁT HIỆN Pb(II)

Trần Thị Thanh Lam¹, Triệu Thị Anh¹, Ma Thị Bình², Trần Quốc Toàn¹, Nguyễn Quốc Dũng¹\* ¹Trường Đại học Sư phạm – ĐH Thái Nguyên, ²Trường Trung học cơ sở Yên Lâm – Tuyên Quang

THÔNG TIN BÀI BÁO		TÓM TẮT				
Ngày nhận bài:	26/6/2025	Trong nghiên cứu này, một quy trình đơn giản và chi phí thấp đã được				
Ngày hoàn thiện:	20/8/2025	phát triển để chế tạo điện cực Co <sub>3</sub> O <sub>4</sub> /ITO bằng phương pháp điện di vật liệu Co(OH) <sub>2</sub> thu được từ kết tủa hóa học dung dịch Co(NO <sub>3</sub> ) <sub>2</sub> , sau đó				
Ngày đăng:	20/8/2025	5 7				
		thành trên nền ITO cho thấy hoạt tính điện hóa tốt trong việc phát hiện				
TỪ KHÓA		Pb(II) trong dung dịch nước. Phương pháp Von-Ampe xung vi phân				
Cobalt oxide Cảm biến điện hóa		được sử dụng để đánh giá hiệu năng cảm biến. Thế tích lũy và thời gian tích lũy được khảo sát hệ thống, với các giá trị tối ưu lần lượt là –0,9 V và 300 giây. Điện cực chế tạo được cho thấy đáp ứng tuyến tính với nồng độ Pb(II) trong khoảng từ 0,1 đến 2 μM, với độ nhạy 35,72				
Pb(II) Đồng kết tủa hóa học Lắng đọng điện di		μA.cm <sup>-2</sup> .μM <sup>-1</sup> và giới hạn phát hiện là 0,047 μM. Kết quả này cho thấy tiềm năng ứng dụng của quy trình chế tạo đơn giản trong phát triển cảm biến điện hóa phát hiện kim loại nặng ở nồng độ vết.				

DOI: https://doi.org/10.34238/tnu-jst.13136

\_\_\_

<sup>\*</sup> Corresponding author. Email: dungnq@tnue.edu.vn

#### 1. Introduction

Heavy metal pollution, particularly from lead ions (Pb(II)), has become a major concern for both human health and the environment due to its high toxicity, bioaccumulation potential, and ability to cause neurological, cardiovascular, and renal dysfunctions [1]. Therefore, the development of rapid, accurate, and sensitive methods for Pb(II) detection is of great importance, especially in environmental monitoring and water quality assessment.

Currently, several traditional analytical techniques are employed for Pb(II) determination, including atomic absorption spectroscopy (AAS), inductively coupled plasma optical emission/mass spectrometry (ICP-OES/ICP-MS), and high-performance liquid chromatography coupled with mass spectrometry (HPLC-MS). While these methods offer high sensitivity and precision, they require expensive instrumentation, complex sample preparation, long analysis times, and unsuitability for on-site measurements [2]. In this context, electrochemical sensing techniques have attracted increasing attention due to their notable advantages such as high sensitivity, low cost, operational simplicity, rapid response, and the ability to detect target ions directly without extensive sample pretreatment [3]. Particularly, when combined with nanostructured functional materials, electrochemical sensors can achieve trace-level detection limits while maintaining good selectivity and stability [4]. As a result, the development of new electrochemical sensor electrodes with high performance and facile fabrication procedures is considered a promising approach in heavy metal analysis.

In recent years, a variety of materials have been investigated to improve the performance of electrochemical sensors for Pb(II) detection [5]. Among them, carbon-based materials such as graphene, graphene oxide (GO), reduced graphene oxide (rGO), and carbon nanotubes (CNTs) have been widely used due to their large surface area, good electrical conductivity, and chemical stability [6]. However, these materials often require surface modification or combination with metals or metal oxides to enhance ion recognition, making the fabrication process more complex [7].

Transition metal oxides such as  $MnO_2$ ,  $SnO_2$ ,  $ZnO_3$ , and particularly cobalt oxide  $(Co_3O_4)$ , have also garnered significant interest due to their flexible redox behavior, high stability, and strong interaction with heavy metal ions [8].  $Co_3O_4$  possesses a spinel structure comprising both  $Co^{2+}$  and  $Co^{3+}$  ions [9], exhibits p-type semiconducting properties, and has shown remarkable electrochemical activity in various sensing applications. In addition,  $Co_3O_4$  is environmentally friendly and can be easily synthesized from common cobalt salts [10].

Although some studies have utilized  $\mathrm{Co_3O_4}$  in combination with conductive materials such as graphene or polypyrrole to enhance sensitivity, most fabrication methods still require complex equipment, electrochemical treatment, or high-temperature processing [11]. Therefore, developing an efficient yet simple electrochemical sensing platform based on  $\mathrm{Co_3O_4}$  using only basic chemical operations is a practical and necessary research direction.

In this study, we propose a facile method to fabricate a Co<sub>3</sub>O<sub>4</sub>/ITO electrode through a three-step process: precipitation of Co(OH)<sub>2</sub> from a Co(NO<sub>3</sub>)<sub>2</sub> solution, electrophoretic deposition onto an ITO substrate, and low-temperature annealing (300 °C) to convert Co(OH)<sub>2</sub> into Co<sub>3</sub>O<sub>4</sub>. The resulting electrode was evaluated for its electrochemical activity using differential pulse anodic stripping voltammetry (DPASV) for the detection of Pb(II), in order to validate the feasibility of the fabrication approach and the sensing performance of the material.

# 2. Experiment

### 2.1. Chemicals and Materials

Cobalt(II) nitrate hexahydrate  $(Co(NO_3)_2 \cdot 6H_2O)$ , sodium hydroxide (NaOH), isopropanol (IPA), and other reagents were all of analytical reagent (AR) grade and used without further purification. ITO-coated glass substrates were cleaned by sequential ultrasonication in acetone, ethanol, and deionized water before use.

# 2.2. Synthesis of Materials

A 0.1 M Co(NO<sub>3</sub>)<sub>2</sub> solution was prepared by dissolving 2.9 g of Co(NO<sub>3</sub>)<sub>2</sub>·6H<sub>2</sub>O in 100 mL of deionized water. Simultaneously, a 0.1 M NaOH solution was prepared by dissolving 2.0 g of NaOH in 500 mL of water. The Co(NO<sub>3</sub>)<sub>2</sub> solution was added dropwise into the NaOH solution under vigorous stirring at room temperature. After stirring for approximately 1 hour, a light pink to bluish precipitate of Co(OH)<sub>2</sub> formed. The precipitate was collected by filtration, thoroughly washed with deionized water until neutral pH was reached, and then dried at 60 °C overnight.

The dried  $Co(OH)_2$  powder was dispersed in isopropanol (IPA) using ultrasonic agitation to obtain a stable suspension. Electrophoretic deposition (EPD) was carried out using a parallel two-electrode setup with ITO substrates placed approximately 1.5 cm apart, under a DC voltage of 30 V for 120 seconds. These parameters were chosen based on preliminary experiments (data not shown), which indicated that lower voltages or shorter deposition times led to insufficient film coverage, while higher voltages or longer times caused non-uniform deposition and poor adhesion. The selected conditions (30 V, 120 s) provided a uniform  $Co(OH)_2$  layer with good adhesion and reproducibility across different samples. For all electrochemical measurements, the working area of the electrode was fixed at  $0.5 \times 0.5$  cm to ensure consistency across experiments. After deposition, the ITO substrates were rinsed with IPA, air-dried, and annealed at 300 °C in ambient air for 2 hours to thermally convert  $Co(OH)_2$  to  $Co_3O_4$ .

# 2.3. Material characterization

The morphology and elemental composition of the synthesized materials were characterized by scanning electron microscopy (SEM) and energy-dispersive X-ray spectroscopy (EDS). The crystal structure of the samples was analyzed using X-ray diffraction (XRD).

#### 2.4. Electrochemical measurements

Electrochemical measurements were performed using a conventional three-electrode system consisting of the  $\text{Co}_3\text{O}_4/\text{ITO}$  working electrode, an Ag/AgCl reference electrode, and a platinum wire counter electrode. Differential pulse anodic stripping voltammetry (DPASV) was employed to evaluate the electrochemical response to Pb(II) in an acetate buffer solution at pH 5. Accumulation potential and time were optimized, and the optimal conditions ( $-0.9\,\text{V}$  accumulation potential and  $300\,\text{s}$  accumulation time) were applied for subsequent measurements.

# 3. Results and discussion

### 3.1. Morphological and elemental characterization

Figure 1 shows the SEM images and corresponding EDS spectra of the  $Co(OH)_2$  precursor (a–b) and the final  $Co_3O_4$  product (c–d) after thermal annealing. As observed in Figure 1.a, the  $Co(OH)_2$  sample consists of aggregated nanosheets with irregular shapes and loosely stacked layers. These nanosheets form a porous, flake-like morphology, which is beneficial for dispersion and electrophoretic deposition. After annealing at 300 °C, the morphology is retained to a large extent (Figure 1.c), but the nanosheets appear denser, with slightly roughened surfaces and enhanced stacking. This change suggests that the  $Co(OH)_2$  precursor has undergone solid-state transformation into  $Co_3O_4$  while partially preserving the initial layered structure.

The EDS analysis confirms the elemental composition of the samples. The  $Co(OH)_2$  material (Figure 1.b) exhibits a Co:O atomic ratio of approximately 1:2 (Co = 33.39 at.%, O = 66.61 at.%), which is consistent with the hydroxide composition. After thermal conversion, the  $Co_3O_4$  sample (Figure 1d) shows an increased cobalt content (Co = 39.15 at.%) and a corresponding decrease in oxygen (O = 60.85 at.%), reflecting the formation of a mixed-valence oxide phase ( $Co^{2+}/Co^{3+}$ ). No peaks of other elements were detected, indicating the high purity of both the precursor and final product.

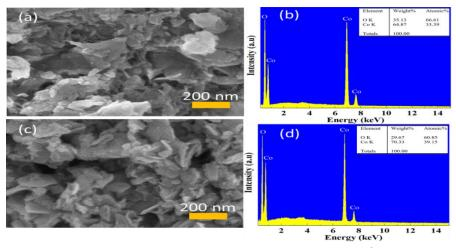


**Figure 1.** SEM images of (a)  $Co(OH)_2$  and (c)  $Co_3O_4$  after annealing at 300 °C, showing retention of porous nanosheet morphology; EDS spectra of (b)  $Co(OH)_2$  and (d)  $Co_3O_4$  confirm elemental composition and successful phase transformation

The combination of SEM and EDS results verifies that the electrophoretic and thermal processing steps successfully transformed the precursor into a Co<sub>3</sub>O<sub>4</sub> nanostructure with retained morphology and appropriate stoichiometry, suitable for electrochemical sensing applications.

The crystal structure of the synthesized  $\text{Co}_3\text{O}_4/\text{ITO}$  electrode was examined by X-ray diffraction (XRD), as shown in Figure 2. The diffraction peaks at  $2\theta \approx 31.2^\circ$ ,  $36.8^\circ$ ,  $44.8^\circ$ ,  $55.8^\circ$ ,  $59.4^\circ$ , and  $65.0^\circ$  correspond to the (220), (311), (400), (422), (511), and (440) planes of spinel-structured  $\text{Co}_3\text{O}_4$ , in good agreement with the standard JCPDS card No. 42-1467. These peaks indicate the successful formation of polycrystalline  $\text{Co}_3\text{O}_4$  with a cubic spinel phase.

In addition to  $\text{Co}_3\text{O}_4$  peaks, several reflections marked with asterisks (\*) at ~30.7°, 35.2°, 50.9°, and 60.6° can be attributed to the underlying ITO substrate (JCPDS No. 39-1058), which are assigned to the (222), (440), (411), and (622) planes of  $\text{In}_2\text{O}_3$ . The presence of these signals confirms that the  $\text{Co}_3\text{O}_4$  layer is relatively thin and allows partial detection of the conductive substrate.

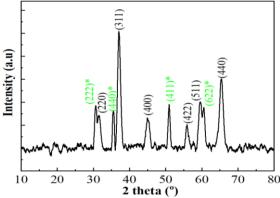


**Figure 2.** XRD pattern of the  $Co_3O_4/TTO$  electrode; Peaks indexed as (220), (311), (400), (422), (511), and (440) confirm the formation of spinel  $Co_3O_4$ (JCPDS No. 42-1467), while peaks marked \* correspond to the ITO substrate (JCPDS No. 39-1058)

No additional peaks corresponding to cobalt hydroxide or other cobalt oxide phases were observed, suggesting complete thermal conversion of  $Co(OH)_2$  to  $Co_3O_4$  and high phase purity of the electrode surface. The well-defined peaks also reflect good crystallinity of the  $Co_3O_4$  nanostructure obtained at a relatively low annealing temperature of 300  $^{\circ}C$ .

# 3.2. Electrochemical performance of the Co<sub>3</sub>O<sub>4</sub>/ITO electrode

The electrochemical behavior of the  $\text{Co}_3\text{O}_4/\text{ITO}$  electrode was investigated using differential pulse anodic stripping voltammetry (DPASV) to optimize measurement conditions and evaluate the accumulation efficiency of  $\text{Pb}^{2+}$  on the electrode surface. All experiments were conducted in acetate buffer solution (pH = 5) containing 0.5  $\mu$ M Pb(II) using a three-electrode system: the  $\text{Co}_3\text{O}_4/\text{ITO}$  working electrode, a Pt counter electrode, and an Ag/AgCl reference electrode.

The accumulation potential plays a critical role in the reduction and enrichment of Pb(II) ions onto the electrode surface. Figure 3.a displays the DPASV responses of  $0.5 \,\mu\text{M}$  Pb(II) under different accumulation potentials: -0.7, -0.8, -0.9, -1.0, and  $-1.1 \,\text{V}$ . As the accumulation potential becomes more negative from -0.7 to  $-0.9 \,\text{V}$ , the peak current near  $-0.55 \,\text{V}$  increases, indicating improved Pb<sup>2+</sup> deposition efficiency on the electrode surface. This behavior is consistent with the electrochemical reduction reaction Pb<sup>2+</sup> + 2e<sup>-</sup>  $\rightarrow$  Pb<sup>0</sup>, where a sufficiently negative potential facilitates the reduction and accumulation of metallic Pb.

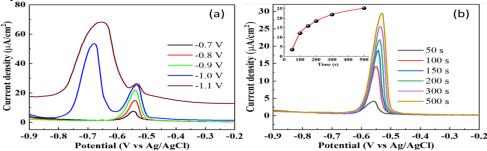


**Figure 3**. (a) DPASV responses of the Co<sub>3</sub>O<sub>4</sub>/ITO electrode toward 0.5 μM Pb(II) at various accumulation potentials (-0.7 to -1.1 V); (b) Responses at different accumulation times (50–500 s); the inset shows the corresponding peak current versus time, indicating saturation beyond 300 s

However, at -1.0 and -1.1 V, new peaks appear in the range of -0.679 to -0.656 V with broader shapes, while the original peak around -0.55 V diminishes or disappears. This phenomenon may be related to structural or redox-state changes of the  $\text{Co}_3\text{O}_4$  material under excessively negative potentials, possibly leading to the formation of intermediate phases or side reactions unfavorable for analytical performance. Repeated measurements at lower potentials (-0.7 to -0.9 V) still show the appearance of this broader peak at -0.656 V, suggesting the change is irreversible. The broad peaks observed at -1.0 V and -1.1 V may be attributed to deep reduction processes that alter the oxide structure or generate intermediate phases, resulting in unstable signals. This observation indicates an irreversible behavior of the electrode material at excessively negative accumulation potentials. Therefore, -0.9 V was selected as the optimal accumulation potential to balance enrichment efficiency and electrode stability.

Accumulation time was then varied from 50 to 700 s at the optimized potential of -0.9 V. As shown in Figure 3b, the stripping peak current of  $Pb^{2+}$  (at  $0.5~\mu M$  concentration) increases with longer accumulation time, especially in the lower time range (<300 s). This is due to the increased amount of reduced Pb being deposited onto the electrode surface, thereby enhancing the oxidation signal during the DPASV scan.

The inset of Figure 3b presents the dependence of peak current density on accumulation time, which shows a saturation trend when time exceeds 300 s. The reduced slope suggests that the electrode surface becomes saturated or undergoes partial restructuring, limiting further Pb accumulation. Based on this, an accumulation time of 300 s was chosen as optimal to ensure a good trade-off between sensitivity, analysis time, and the stability of the Co<sub>3</sub>O<sub>4</sub> sensing layer.

#### 3.3. Calibration curve and detection limit

After optimizing the experimental parameters (accumulation potential of  $-0.9\,V$  and accumulation time of 300 s), the  $Co_3O_4/ITO$  electrode was employed to construct a calibration curve for Pb(II) detection using DPASV. Measurements were conducted in acetate buffer (pH 5) containing varying concentrations of Pb(II), ranging from 0.01 to 20  $\mu M$ .

As shown in Figure 4.a, the stripping peak current increases with rising Pb<sup>2+</sup> concentrations, indicating a good electrochemical response of the sensor. Additionally, a slight positive shift in peak potential is observed at higher concentrations, which may be attributed to the increased accumulation of Pb on the electrode surface, requiring a more positive potential for complete

oxidation. Moreover, broadening of the peak at higher concentrations suggests a slower reoxidation process of metallic Pb, likely due to mass transport limitations or saturation of the electrode surface.

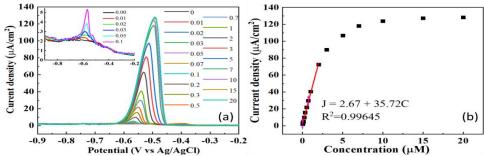


**Figure 4.** (a) DPASV curves of the  $Co_3O_4/ITO$  electrode at different Pb(II) concentrations ranging from 0.01 to 20  $\mu$ M; (b) Calibration curve with linear regression for Pb(II) in the range 0.01–1.0  $\mu$ M: J=2.67+35.72C,  $R^2=0.99645$ 

**Table 1.** Comparative performance of representative electrochemical sensors for Pb(II) detection using various transition metal oxides

Electrode material	LOD (μg/L)	Linear range (μg/L)	Measurement conditions	Method	Reference
Co <sub>3</sub> O <sub>4</sub> (MOF-derived)	9.77	103.5-310.5	Acetate buffer, pH 5.0	SWASV	[12]
Co <sub>3</sub> O <sub>4</sub> /rGO/PEI	1.13	~200–2070 (estimated)	Acetate buffer, pH 5.0	SWV	[13]
Co <sub>3</sub> O <sub>4</sub> @rGO	0.16	20.7–9315	River water sample (natural matrix)	SWASV	[14]
ZnO/L-cysteine	0.397	10-140	Not specified	SWASV	[15]
Sn/SnO <sub>2</sub>	2.15	6.2–20.7	Bottled drinking water (no pH control)	SWASV	[16]
PIN/Mn <sub>2</sub> O <sub>3</sub> /PANI	0.05	0.05-450	Neutral pH buffer (approx. pH 7)	DPASV	[17]
Co <sub>3</sub> O <sub>4</sub> /ITO (this work)	0.98	2.07 - 207	Acetate buffer, pH 5.0	DPASV	This study

The plot of peak current density versus Pb<sup>2+</sup> concentration is shown in Figure 4.b. A linear relationship was obtained in the concentration range from 0.01 to 1.0  $\mu$ M, which can be described by the regression equation: I = 2.67 + 35.72C,  $R^2 = 0.99645$ ;

where J is the peak current density ( $\mu A$  cm<sup>-2</sup>) and C is the Pb<sup>2+</sup> concentration ( $\mu M$ ). The sensitivity of the sensor, defined by the slope of the linear region, was calculated to be 35.72  $\mu A$  cm<sup>-2</sup>  $\mu M^{-1}$ . The limit of detection (LOD), calculated using the formula LOD =  $3\sigma/S$  (where  $\sigma$  is the standard deviation of the blank signal and S is the slope), was determined to be 0.0047  $\mu M$ . These results confirm the excellent sensitivity and trace-level detection capability of the Co<sub>3</sub>O<sub>4</sub>/ITO electrode for Pb<sup>2+</sup> ions.

# 3.4. Electrode stability and selectivity

The operational stability of the  $\text{Co}_3\text{O}_4/\text{ITO}$  electrode was assessed by performing ten consecutive DPASV measurements at a fixed Pb(II) concentration (0.5  $\mu$ M). As shown in Figure 5.a, the peak current density remained nearly unchanged, with only slight fluctuations between 25.3 and 25.7  $\mu$ A cm<sup>-2</sup>. This result indicates that the electrode maintains good electrochemical stability and reproducibility over multiple cycles, which is crucial for real-world applications.

Selectivity is another important criterion in evaluating electrochemical sensors. To investigate this aspect, a mixed solution containing four heavy metal ions — Cd(II), Pb(II), Cu(II), and Hg(II)—was analyzed under the optimized conditions. As illustrated in Figure 6b, well-separated and distinguishable peaks were observed at approximately –0.75 V, –0.55 V, 0.00 V, and 0.32 V, corresponding to Cd(II), Pb(II), Cu(II), and Hg(II), respectively. The clear peak separation

http://jst.tnu.edu.vn 446 Email: jst@tnu.edu.vn

demonstrates the sensor's capability for simultaneous detection of multiple heavy metal ions without interference, confirming the excellent selectivity of the Co<sub>3</sub>O<sub>4</sub>/ITO electrode.

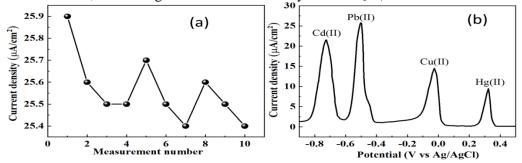


**Figure 5.** (a) Stability of the Co<sub>3</sub>O<sub>4</sub>/ITO electrode evaluated by measuring the peak current response to 0.5 μM Pb(II) over 10 consecutive DPASV cycles under identical conditions; (b) Simultaneous detection of Cd(II), Pb(II), Cu(II), and Hg(II) ions (each at 0.5 μM) by the Co<sub>3</sub>O<sub>4</sub>/ITO electrode using DPASV, demonstrating the selectivity and signal separation capability of the sensor

The chemical and thermal stability of  $Co_3O_4$  in mildly acidic environments (pH  $\approx$  5) has been well-documented in previous studies. For instance, Co<sub>3</sub>O<sub>4</sub> has been fabricated for the detection of Pb(II) at pH 5 [18], yielding a sensitivity of 71.57 μA.μM<sup>-1</sup> and a limit of detection (LOD) of 0.018 uM. Similarly, Co<sub>3</sub>O<sub>4</sub> nanosheets deposited on ITO electrodes applied to the anodic-stripping voltammetric detection of lead ions (Pb<sup>2+</sup>) were tested specifically at pH 5.0, achieving a detection limit of ~0.52 µg.L<sup>-1</sup> and excellent reproducibility during repeated measurements [19]. Co<sub>3</sub>O<sub>4</sub> (MOF-derived) was also used to detect Pb<sup>2+</sup> and Cu<sup>2+</sup> in pH 5 [12]. Additionally, a Co<sub>3</sub>O<sub>4</sub>/rGO–PEI (polyethylenimine) hybrid sensor was used to simultaneously detect multiple heavy metal ions (Cd<sup>2+</sup>, Pb<sup>2+</sup>, Cu<sup>2+</sup>) in an acidic buffer (pH 4–5), and likewise retained high sensitivity and selectivity under these conditions [13]. Taken together, these findings clearly indicate that Co<sub>3</sub>O<sub>4</sub> retains its chemical robustness and electrochemical activity in mildly acidic media (pH  $\leq$  5), proving it is a viable and reliable material for heavy-metal ion sensing in such environments. In this study, an acetate buffer at pH = 5 was employed, providing a suitable environment for both heavy metal ion preconcentration and well-resolved peak separation, while also preserving the chemical integrity of the Co<sub>3</sub>O<sub>4</sub>/ITO electrode. The stability observed in repeatability and reusability tests (Figure 5.a) further supports the durability of the electrode under working conditions, indicating no significant material degradation or activity loss throughout the measurements.

# 4. Conclusion

The present work introduced a straightforward and low-cost route to fabricate a  $\text{Co}_3\text{O}_4/\text{ITO}$  electrode using sequential chemical precipitation, electrophoretic deposition, and mild thermal annealing. The resulting nanostructured  $\text{Co}_3\text{O}_4$  exhibited favorable crystallinity and morphology that enabled efficient Pb(II) detection using DPASV. The sensor achieved excellent analytical figures of merit, including low detection limits and high sensitivity, under optimized conditions. Notably, the fabrication process requires only simple equipment and mild conditions, making it accessible for practical deployment. These findings underscore the potential of the  $\text{Co}_3\text{O}_4/\text{ITO}$  electrode as a reliable and scalable platform for monitoring heavy metal contaminants in aqueous environments. These promising findings lay the groundwork for further fine-tuning of material properties and measurement protocols to improve sensitivity and reproducibility under controlled laboratory conditions.

# REFERENCES

[1] I.R. Chowdhury, S. Chowdhury, M. A. J. Mazumder, and A. Al-Ahmed, "Removal of lead ions (Pb<sup>2+</sup>) from water and wastewater: a review on the low-cost adsorbents," *Applied Water Science*, vol. 12, no. 8, 2022, Art. no. 185.

- [2] Y. Liu, Q. Xue, C. Chang, R. Wang, Z. Liu, and L. He, "Recent progress regarding electrochemical sensors for the detection of typical pollutants in water environments," *Analytical Sciences*, vol. 38, no. 1, pp. 55-70, 2022.
- [3] J. Baranwal, B. Barse, G. Gatto, G. Broncova, and A. Kumar, "Electrochemical sensors and their applications: A review," *Chemosensors*, vol. 10, no. 9, 2022, Art. no. 363.
- [4] A. Uçar, G.A. Tığ, and E. Er, "Recent advances in two dimensional nanomaterial-based electrochemical (bio) sensing platforms for trace-level detection of amino acids and pharmaceuticals," *TrAC Trends in Analytical Chemistry*, vol. 162, 2023, Art. no. 117027.
- [5] B. Mohan, R. Kadiyan, K. Singh, G. Singh, K. Kumar, H. K. Sharma, and A. J. Pombeiro, "MOFs composite materials for Pb<sup>2+</sup> ions detection in water: recent trends & advances," *Microchemical Journal*, vol. 190, 2023, Art. no. 108585.
- [6] A. Razaq, F. Bibi, X. Zheng, R. Papadakis, S. H. M. Jafri, and H. Li, "Review on graphene-, graphene oxide-, reduced graphene oxide-based flexible composites: From fabrication to applications," *Materials*, vol. 15, no. 3, 2022, Art. no. 1012.
- [7] J. M. George, A. Antony, and B. Mathew, "Metal oxide nanoparticles in electrochemical sensing and biosensing: a review," *Microchimica Acta*, vol. 185, 2018 Art. no. 358.
- [8] R. Meng, Q. Zhu, T. Long, X. He, Z. Luo, R. Gu, W. Wang, and P. Xiang, "The innovative and accurate detection of heavy metals in foods: A critical review on electrochemical sensors," *Food Control*, vol. 150, 2023, Art. no. 109743.
- [9] C. Anuradha and J. Jeyanthi, "Comprehensive study of structural, optical, electrical, and magnetic properties of cobalt oxide nanoparticles synthesized via curd-based biogenic approach," *Applied Physics A*, vol. 131, no. 4, pp. 1-12, 2025, Art. no. 301.
- [10] H. Hu, L. Wang, and X. Zhou, "A Novel Electrochemical Sensor for Arsenic Detection with High Sensitivity and Stability Based on Sulfur-Doped Co<sub>3</sub>O<sub>4</sub> Nanocomposites," SSRN 5052260, 2024, doi: 10.2139/ssrn.5052260.
- [11] M. N. Muhammad-Hashami, A. R. Seitkazinova, A. R. Kerimkulova, A. S. Beisebayeva, T. Mashan, and N. Nurmukhanbetova, "Synthesis of Co<sub>3</sub>O<sub>4</sub> Nanoparticles through Solution Combustion Method and Their Applications: A Review," *Preprints*, 2024, doi: 10.20944/preprints202403.1118.v1.
- [12] J. Guo, J. Li, X. Xing, W. Xiong, and H. Li, "Development of MOF-derived Co<sub>3</sub>O<sub>4</sub> microspheres composed of fiber stacks for simultaneous electrochemical detection of Pb<sup>2+</sup> and Cu<sup>2+</sup>," *Microchimica Acta*, vol. 191, no. 9, 2024, Art. no. 542.
- [13] A.U. Rehman, M. Fayaz, H. Lv, Y. Liu, J. Zhang, Y. Wang, L. Du, R. Wang, and K. Shi, "Controllable synthesis of a porous PEI-functionalized Co<sub>3</sub>O<sub>4</sub>/rGO nanocomposite as an electrochemical sensor for simultaneous as well as individual detection of heavy metal ions," *ACS omega*, vol. 7, no. 7, pp. 5870-5882, 2022.
- [14] J. You, J. Li, Z. Wang, M. Baghayeri, and H. Zhang, "Application of Co<sub>3</sub>O<sub>4</sub> nanocrystal/rGO for simultaneous electrochemical detection of cadmium and lead in environmental waters," *Chemosphere*, vol. 335, 2023, Art. no 139133.
- [15] V. H. Oliveira, F. Rechotnek, E. P. da Silva, V. de S. Marques, A. F. Rubira, R. Silva, S. A. Lourenco, and E. C. Muniz, "A sensitive electrochemical sensor for Pb<sup>2+</sup> ions based on ZnO nanofibers functionalized by L-cysteine," *Journal of Molecular Liquids*, vol. 309, 2020, Art. no. 113041.
- [16] S. Kumar, P. P. Singh, A. K. Arya, D. Sur, and S. Kaushal, "SnO<sub>2</sub>/SnSbP nanocomposite–based ion-selective electrode for the trace level sensing of Pb<sup>2+</sup> ions in waste water samples," *Ionics*, vol. 31, pp. 5055–5066, 2025.
- [17] A. Yousefi, H. Aghaie, M. Giahi, and L. Maleknia, "Determination of Cd<sup>2+</sup> and Pb<sup>2+</sup> by polyindole/Mn<sub>2</sub>O<sub>3</sub> nanocomposite and polyindole/Mn<sub>2</sub>O<sub>3</sub>/polyaniline nanofibers modified glassy carbon electrode," *Chemical Papers*, vol. 77, no. 2, pp. 733-743, 2023.
- [18] Z.-G. Liu, X. Chen, J.-H. Liu, and X.-J. Huang, "Well-arranged porous Co<sub>3</sub>O<sub>4</sub> microsheets for electrochemistry of Pb (II) revealed by stripping voltammetry," *Electrochemistry Communications*, vol. 30, pp. 59-62, 2013.
- [19] L. Yu, P. Zhang, H. Dai, L. Chen, H. Ma, M. Lin, and D. Shen, "An electrochemical sensor based on Co<sub>3</sub>O<sub>4</sub> nanosheets for lead ions determination," *RSC Advances*, vol. 7, no. 63, pp. 39611-39616, 2017.